The Astrophysical Journal, 760:144 (8pp), 2012 December 1 doi:10.1088/0004-637X/760/2/144

THERMAL AND CHEMICAL STRUCTURE VARIATIONS IN TITAN'S STRATOSPHERE DURING THE *CASSINI* MISSION

Georgios Bampasidis[1,2], A. Coustenis[1], R. K. Achterberg[3], S. Vinatier[1], P. Lavvas[4], C. A. Nixon[5], D. E. Jennings[5], N. A. Teanby[6], F. M. Flasar[5], R. C. Carlson[5,7], X. Moussas[2], P. Preka-Papadema[2], P. N. Romani[5], E. A. Guandique[5,8], and S. Stamogiorgos[2]

[1] Laboratoire d'Études Spatiales et d'Instrumentation en Astrophysique (LESIA), Observatoire de Paris, CNRS, UPMC Univ. Paris 06, Univ. Paris-Diderot, 5, place Jules Janssen, F-92195 Meudon Cedex, France; gbabasid@phys.uoa.gr
[2] Faculty of Physics, National and Kapodistrian University of Athens, Panepistimioupolis, GR 15783 Zographos, Athens, Greece
[3] Department of Astronomy, University of Maryland, College Park, MD 20742, USA
[4] GSMA, Université Reims Champagne-Ardenne, F-51687 Reims Cedex 2, France
[5] Goddard Space Flight Center, Greenbelt, MD 20771, USA
[6] School of Earth Sciences, University of Bristol, Bristol BS8 1RJ, UK
[7] IACS, Catholic University of America, and NASA/Goddard Space Flight Center, USA
[8] Adnet Systems, Inc., Rockville, MD, USA
Received 2012 September 8; accepted 2012 October 8; published 2012 November 16

ABSTRACT

We have developed a line-by-line Atmospheric Radiative Transfer for Titan code that includes the most recent laboratory spectroscopic data and haze descriptions relative to Titan's stratosphere. We use this code to model *Cassini* Composite Infrared Spectrometer data taken during the numerous Titan flybys from 2006 to 2012 at surface-intercepting geometry in the 600–1500 cm^{-1} range for latitudes from 50°S to 50°N. We report variations in temperature and chemical composition in the stratosphere during the *Cassini* mission, before and after the Northern Spring Equinox (NSE). We find indication for a weakening of the temperature gradient with warming of the stratosphere and cooling of the lower mesosphere. In addition, we infer precise concentrations for the trace gases and their main isotopologues and find that the chemical composition in Titan's stratosphere varies significantly with latitude during the 6 years investigated here, with increased mixing ratios toward the northern latitudes. In particular, we monitor and quantify the amplitude of a maximum enhancement of several gases observed at northern latitudes up to 50°N around mid-2009, at the time of the NSE. We find that this rise is followed by a rapid decrease in chemical inventory in 2010 probably due to a weakening north polar vortex with reduced lateral mixing across the vortex boundary.

Key words: infrared: planetary systems – planets and satellites: atmospheres – planets and satellites: composition – planets and satellites: individual (Titan) – radiation mechanisms: thermal – radiative transfer

Online-only material: color figures

1. CONTEXT AND OBSERVATIONS

Latitudinal variations in Titan's stratospheric thermal and chemical structure have been reported in the past from *Cassini* data acquired by the Composite Infrared Spectrometer (CIRS) (Flasar et al. 2005; Teanby et al. 2006; Coustenis et al. 2007, 2008, 2010; de Kok et al. 2007; Teanby et al. 2007, 2008, 2009a; Vinatier et al. 2007, 2010; Nixon et al. 2008a; Achterberg et al. 2008, 2011). Here, we explore the thermal and chemical evolution discernible within the timeframe from 2006 to 2012, thus complementing and refining previous reports from earlier stages of the mission. We study Titan's neutral atmosphere between ∼120 and 300 km in altitude (the stratosphere and lower mesosphere) and latitudes from 50°S to 50°N.

CIRS is a Fourier Transform Spectrometer, aboard the *Cassini* orbiter, consisting of two interferometers probing the far-infrared (10–600 cm^{-1}) and mid-infrared (600–1500 cm^{-1}) ranges with an apodized spectral resolution varying from 15.5 to 0.5 cm^{-1}. CIRS scans Titan's atmosphere through three separate focal planes that share the same telescope: FP1 (10–600 cm^{-1}), FP3 (600–1100 cm^{-1}), and FP4 (1100–1500 cm^{-1}) (Flasar et al. 2004). We focus here mainly on FP3 and FP4 high-resolution observations (0.5 cm^{-1}) but also some medium resolution ones (2.5 cm^{-1}).

Prior to 2006 (flybys T0–T9) insufficient data at the right conditions for our purposes (signal-to-noise, emission angle, distance, region, etc.) were acquired. During the flybys that followed, CIRS obtained a large number of spectra in FP3 and FP4 at high, medium, and low spectral resolutions (0.53, 2.54, and 15 cm^{-1}), respectively, in surface-intercepting (nadir) and horizontal viewing (limb) geometry conditions, albeit not always covering all latitudes, so that in the northern hemisphere we have data only from late 2007 to 2010. An instrument anomaly followed by a reboot of CIRS took place in December 2006, thus depriving us of data from that time. We otherwise use all available and exploitable data at high spectral resolution (0.5 cm^{-1}) and perform averages of the spectra acquired during one or several flybys as necessary to attain a high signal-to-noise ratio for our calculations.

Tables 1 and 2 list the CIRS FP3 nadir northern and southern averages, respectively, at high resolution (0.5 cm^{-1}), while Tables 3 and 4 list the associated FP4 averages. The average signal-to-noise ratio is shown as well as the corresponding *Cassini* Titan flyby(s) and the relative solar longitude (Ls). The selections we made in order to enhance the signal-to-noise ratio cover different latitudes on Titan (we sum all longitudes because no longitudinal variations were found in our studies; Coustenis et al. 2007, 2010). The averaged spectra created from the high-resolution nadir data in the several latitudinal bins (between 50°S and 50°N) contain a large number of spectra in general, with some exceptions (as indicated in Tables 1–4). As discussed in Coustenis et al. (2007), we have taken care to correct the

Table 1
Titan Flybys and FP3 Data Acquisition Characteristics from 2007 March to 2011 September Averaged in Northern Latitudinal Bins

Year	Month	Latitude	Total Number of Spectra	Signal-to-noise	Airmass	*Cassini* Flyby	Ls (°)
2007	Mar	50°N	357	18.6	1.02	T26–T27	329
“	Dec	50°N	335	19.9	1.25	T38–T39	338–339
2008	Feb–Mar–Jul	50°N	145	12.4	1.19	T41–T45	341–347
2009	Mar	50°N	517	25	1.35	T51	355
“	Apr–May	50°N	275	15.3	1.01	T52–T55	355–357
“	Jun	50°N	476	25.6	1.88	T56–T57	358
2010	Jan	50°N	284	21.3	1.69	T65–T66	005–006
2006	Jul	30°N	551	34	1.17	T15–T17	320
2007	May	28°N	934	44.7	1.06	T30–T31	331–332
“	Dec	31°N	905	45.4	1.14	T38–T39	338–339
2008	Mar	30°N	992	42.3	1.01	T42	342
“	Dec	36°N	262	20.5	1.03	T48–T49	351–352
2009	Dec	30°N	748	44.5	1.46	T63–T64	004–005
2010	Jun	35°N	599	37.4	1.24	T69–T70	010
2011	Sep	32°N	771	46.8	1.49	T78	025
2006	Jan	1°N	1291	56.2	1.01	T10	314
“	Jul	1°N	2118	71.8	1.01	T15–T16	320
2007	Apr–May	1°N	189	23.9	1.21	T28–T29	330–331
“	Jun	1°N	1497	62.5	1.06	T32–T33	332–333
“	Aug	1°N	152	19.3	1.01	T35	335
2008	Jan	1°N	589	39.4	1.07	T40	340
“	May	2°N	597	47	1.55	T43–T44	344–345
2009	Mar–Jul	1°N	86	18.3	1.75	T51–T59	355
“	Oct	1°N	72	14.9	1.19	T62	002
“	Dec	1°N	283	25.6	1.01	T63–T64	004
2010	Sep	3°N	1504	58.9	1.02	T72	014
2011	May	11°N	921	50	1.20	T76	021

Table 2
Titan Flybys and FP3 Data Acquisition Characteristics from 2006 February to 2012 January Averaged in Southern Latitudinal Bins

Year	Month	Latitude	Total Number of Spectra	Signal-to-noise	Airmass	*Cassini* Flyby	Ls (°)
2006	Mar	1°S	1515	61.3	1.04	T12	316
2007	Oct	1°S	93	17	1.28	T19–T20	323–324
“	Jul	1°S	232	23.3	1.01	T34	334
“	Nov	1°S	813	44.5	1.01	T37	338
“	Dec	3°S	276	25.3	1.01	T38–T39	338–339
2008	Feb	1°S	426	39.8	1.46	T41	341
2010	Apr–May	1°S	466	33.0	1.01	T67	008
“	Jun	1°S	391	30.6	1.02	T69–T70	010
“	Jul	1°S	985	49.8	1.08	T71	011
2011	Dec	2°S	1047	52.1	1.19	T79	028
2006	Feb	30°S	666	37.7	1.88	T11	315
“	May	30°S	536	35.3	1.33	T14	318
2008	Nov	38°S	1055	39.9	1.02	T46–T47	350–351
2009	Dec	24°S	961	40	1.08	T63–T64	004–005
2010	May	24°S	911	44.9	1.30	T68	009
2012	Jan	30°S	1980	56.1	1.49	T80–T81	029
2006	Oct	50°S	568	30.9	1.18	T19–T20	323
2007	Jan	50°S	925	37.0	1.04	T23–T24	327
“	Mar–May	50°S	341	28.2	1.64	T26–T31	329–332
“	Jul–Aug	50°S	647	39.6	1.70	T34–T35	334
“	Dec	50°S	467	31.7	1.53	T38–T39	338–339
2008	Jul	50°S	34	9.6	1.28	T41	341
2009	Mar	50°S	198	17.2	1.09	T51	355
“	May	50°S	1288	45.2	1.25	T54–T55	357
2010	Apr	50°S	124	16.0	1.69	T67	008

data for any latitude smearing effect observed for high emission angles and/or data taken at latitudes higher than 50°N. So that the latitudes sounded can be about 5° lower when the line of sight intercepts the surface at 55°N or 55°S, the actual latitude at the vertical of the stratospheric altitudes being observed is then rather 50°N and 50°S, respectively. The latitudes listed in the tables are corrected for this effect.

We have applied a radiative transfer code to analyze the CIRS data spanning the 2006–2012 timeline, during which the *Cassini* mission performed 71 Titan flybys (Tables 1–4). Besides the

Table 3
Titan Flybys and FP4 Data Acquisition Characteristics from 2007 March to 2011 September Averaged in Northern Latitudinal Bins

Year	Month	Latitude	Total Number of Spectra	Signal-to-noise	Airmass	*Cassini* Flyby	Ls (°)
2007	Mar	50°N	1376	64.6	1.03	T26–T27	329
“	Dec	50°N	342	34.4	1.26	T38–T39	338–339
2008	Feb–Mar–Jul	50°N	166	12.8	1.14	T41–T45	341–347
2009	Mar	50°N	417	30	1.28	T51	355
“	Apr–May	50°N	1481	49.9	1.01	T52–T55	355–357
“	Jun	50°N	575	35.8	1.65	T56–T57	358
2010	Jan	50°N	234	27.6	1.67	T65–T66	005–006
2006	Jul	30°N	567	67.1	1.17	T15–T16	320
2007	May	30°N	1789	125	1.06	T30–T31	331–332
“	Dec	30°N	657	81.8	1.18	T38–T39	338–339
2008	Mar	30°N	1013	86.5	1.02	T42	342
“	Dec	35°N	394	74.1	1.03	T48–T49	351–352
2009	Dec	30°N	764	83.9	1.36	T63–T64	004–005
2010	Jun	36°N	503	69.6	1.25	T69–T70	010
2011	Sep	28°N	1107	106	1.39	T78	025
2006	Jan	2°N	869	107.3	1.01	T10	314
“	Jul	1°N	1840	152.0	1.01	T15–T16	320
2007	Apr–May	3°N	93	37.5	1.20	T28–T29	330–331
“	Jul	1°N	198	51.9	1.02	T34	334
“	Aug	1°N	146	45.5	1.02	T35	335
2008	Jan	1°N	449	80.3	1.09	T40	340
“	Feb	1°N	439	86.2	1.59	T41	341
“	May	3°N	64	32.9	1.70	T43–T44	344–345
2009	Dec	1°N	322	64.8	1.03	T63–T64	004
2010	Apr–May	1°N	233	54.1	1.01	T67	008
2011	May	7°N	765	99.8	1.18	T76	021

Table 4
Titan Flybys and FP4 Data Acquisition Characteristics from 2006 February to 2012 January Averaged in Southern Latitudinal Bins

Year	Month	Latitude	Total Number of Spectra	Signal-to-noise	Airmass	*Cassini* Flyby	Ls (°)
2006	Mar	1°S	1515	142.1	1.09	T12	316
“	Oct	1°S	96	39.4	1.26	T19–T20	323–324
2007	Jun	1°S	2545	195.1	1.09	T32–T33	332–333
“	Nov	1°S	869	106.7	1.01	T37	338
“	Dec	1°S	382	70.9	1.02	T38–T39	338–339
2009	Mar–Jul	1°S	84	39.2	1.71	T51–T59	355
“	Oct	1°S	60	26.6	1.09	T62	002
2010	Jun	1°S	367	69.4	1.01	T69–T70	010
“	Jul	1°S	913	110.8	1.13	T71	011
“	Sep	3°S	1622	136.9	1.01	T72	014
2011	Dec	10°S	1866	157	1.24	T79	028
2006	Feb	30°S	666	96	1.21	T11	315
“	May	30°S	551	85.5	1.26	T14	318
2008	Nov	31°S	1055	106.4	1.01	T46–T47	350–351
2009	Dec	28°S	980	103.4	1.12	T63–T64	004–005
2010	May	24°S	1028	114.3	1.21	T68	009
2012	Jan	30°S	2083	133.8	1.15	T80–T81	029
2006	Oct	50°S	546	78.8	1.16	T19–T20	323
2007	Jan	50°S	842	95.8	1.07	T23–T24	327
“	Mar–May	50°S	320	63.1	1.42	T26–T31	329
“	Jul–Aug	50°S	538	86.8	1.68	T34–T35	334
“	Dec	50°S	456	77.5	1.59	T38–T39	338–339
2008	Jul	50°S	51	25.6	1.62	T41	341
2009	Mar	50°S	584	73.4	1.13	T51	355
“	May	50°S	892	91.0	1.33	T54–T55	357
2010	Apr	50°S	525	35.4	1.71	T67	008

high resolution spectra, we also have analyzed six data sets at medium resolution (2.54 cm^{-1}) taken in FP3 and FP4 in January 2008 (flyby T40), April 2009 (flybys T52–T53), and May 2010 (flyby T68). They contain 459, 1193, and 160 spectra each in FP3 and a similar or higher number in the FP4. Each selection at high or medium spectral resolution was restricted to emission angles lower than 65° for optimum radiative transfer treatment.

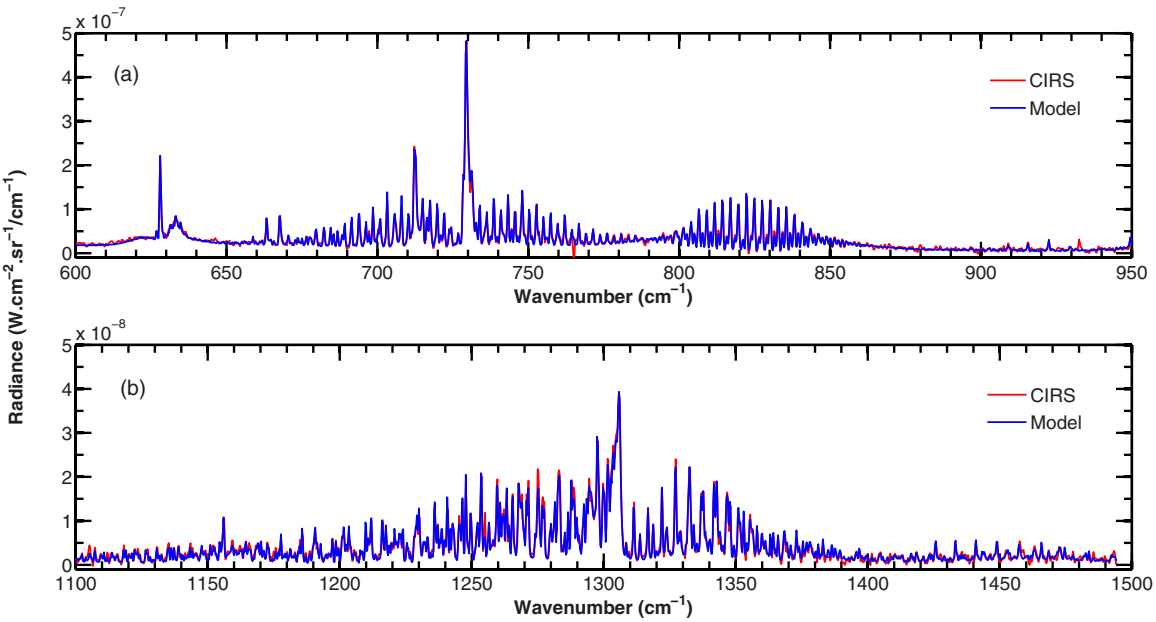

Figure 1. Example of fit of the FP3 (a) and FP4 (b) spectrum of Titan taken by *Cassini* CIRS in June 2009 at flybys T56–T57 at 50°N, containing 476 spectra for FP3 and 575 spectra for FP4.

(A color version of this figure is available in the online journal.)

2. DATA ANALYSIS

The *Cassini*/CIRS spectra are analyzed using a method extensively described in previous articles (Coustenis et al. 2007, 2010). In brief, we model Titan's thermal infrared spectrum by use of a line-by-line monochromatic radiative transfer code updated from the one we used in previous Titan atmospheric structure retrievals (Coustenis et al. 2010, and references therein). In this new release (ARTT, for Atmospheric Radiative Transfer for Titan), we have included more constituents relevant to Titan's chemistry (26 species in total, all the so-far detected hydrocarbons, nitriles, and oxygen compounds in addition to the main molecules N_2, H_2, CH_4, and argon). Our list of molecules includes in particular the $^{13}CH_4$, $^{13}CH_3D$, $^{12}C^{13}CH_2$, and $H^{15}CN$ isotopologues which are essential in fitting the emission bands of methane, acetylene, and hydrogen cyanide and allow us to infer the $^{12}C/^{13}C$ and $^{14}N/^{15}N$ ratios. Furthermore, new oxygen and hydrocarbon isotopologues as detected by Jennings et al. (2008) and Nixon et al. (2008b) are included. Spectroscopic parameters for the molecules found in the FP3 and FP4 spectral ranges are from GEISA 2009 (Jacquinet-Husson et al. 2011) and HITRAN 2008 (Rothman et al. 2009) databases, with several updates, as for instance in the case of ethane and propane, both of which are simulated from the individual line lists of Vander Auwera et al. (2007) and Flaud et al. (2010), respectively.

We first retrieve temperature profiles by the inversion of the observed ν_4 methane emission band at 1305 cm^{-1} in CIRS FP4 following the method described in Achterberg et al. (2008, 2011). We use the CH_4 vertical mixing ratio profile in the stratosphere as measured by the Huygens probe (Niemann et al. 2010) and compatible with the CIRS inferences from FP1 (Flasar et al. 2005), which yields 1.48% above the cold trap.

The initial guess temperature profile for these calculations was the 15°S profile from Flasar et al. (2005), in a process described in detail in Achterberg et al. (2008). We also made tests using the HASI measured temperature structure in the stratosphere and troposphere (Fulchignoni et al. 2005), as discussed in the next section. We then use the temperature profiles to solve the radiative transfer equation in the FP3 part of the spectrum for the mixing ratios of the various components seen in emission at different epochs and latitudes (Tables 1 and 2).

For all the molecules analyzed here in "nadir" geometry conditions, we adopt constant-with-height profiles above the condensation level relevant to stratospheric levels of 0.1–20 mbar essentially (roughly 80–280 km). As explained in detail in Section 4.4 of Coustenis et al (2010), the use of constant vertical profiles does not allow for a good fit of the whole C_2H_2 emission band centered at 729 cm^{-1}. We therefore first derive the C_2H_2 abundance that fits the Q-branch and then adjust the fit in the wings of the band to infer the other mixing ratios of the weaker species in the 620–780 cm^{-1} region. In order to model the continuum observed in the spectra, we have used the haze dependence as reported in Vinatier et al. (2012a) giving the aerosol refractive index from CIRS spectra in the far- and mid-infrared regions near 15°S and 20°S, adjusted to match the level of radiance observed in between the molecular bands in our selections.

3. TEMPERATURE EVOLUTION OF TITAN'S STRATOSPHERE DURING THE *CASSINI* MISSION

Figure 1 shows an example of fits obtained in the FP3 (600–1000 cm^{-1}) region and in the FP4 (1100–1500 cm^{-1}) region. The latter is used for all spectral selections to derive the corresponding temperature profile.

Figures 2(a)–(d) show the results of the temperature as a function of latitude, using the altitude information contained in the resolved lines of the ν_4 methane band. Figures 2(a) and (b) (upper panel) show the temperature structure inferred at two latitudes (50°N and 30°N) at certain dates during the *Cassini* mission. The temperature profiles discussed hereafter were calculated using as an initial guess the one from Flasar et al. (2005).

But we have also run tests using thermal profiles retrieved from the same CIRS FP4 selections but by adopting into the

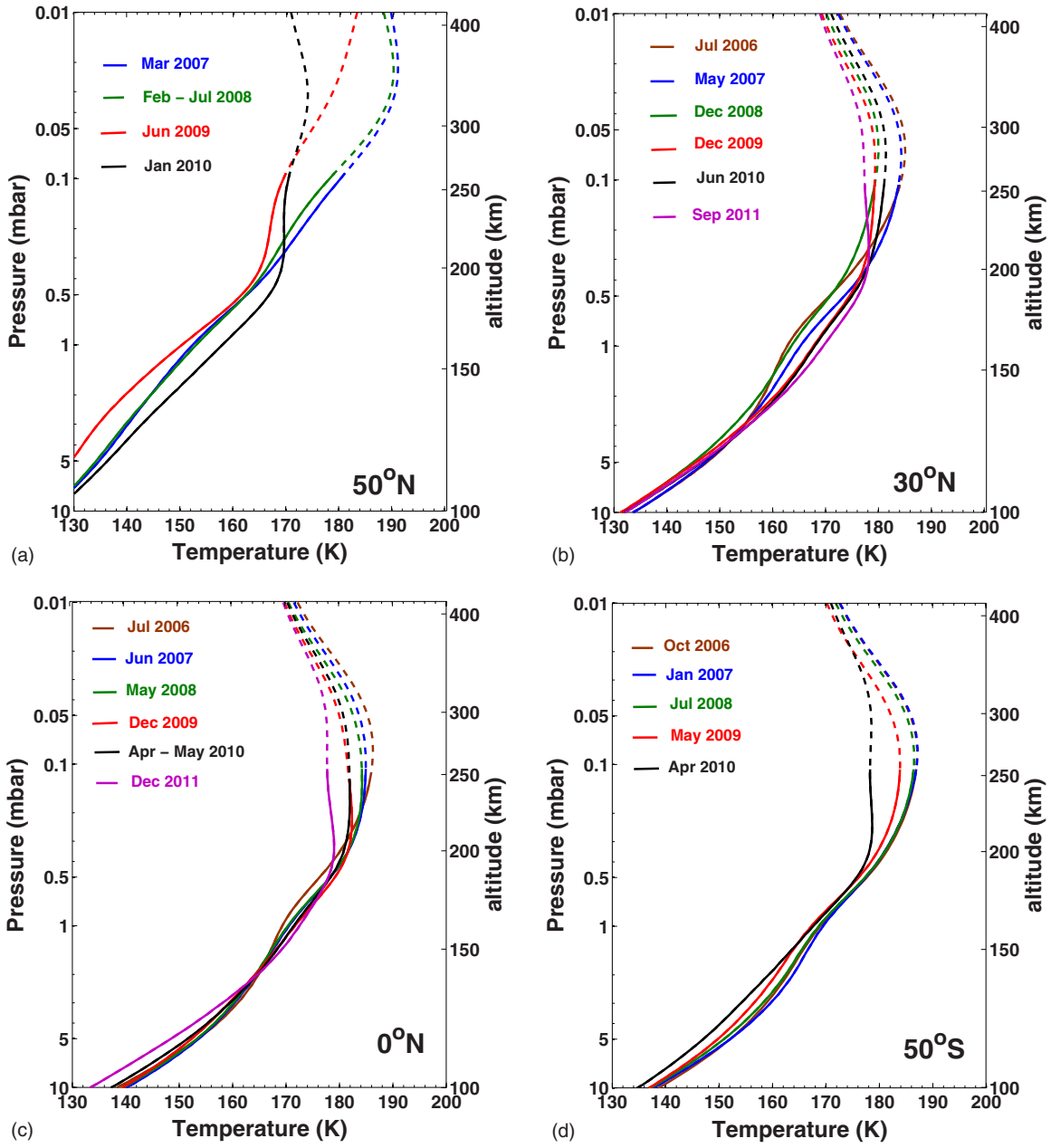

Figure 2. Retrieved thermal profiles from CIRS nadir data at (a) 50°N, (b) 30°N, (c) equator, and (d) 30°S. The typical error bar uncertainty is about 0.7 K at 1 mbar and at most 4 K at 5 mbar. Dashed lines indicate the altitude levels above which the temperature has higher uncertainties.

(A color version of this figure is available in the online journal.)

constrained inversion algorithm (Achterberg et al. 2008) as the a priori reference profile the HASI temperature structure (Fulchignoni et al. 2005). We find that at the equatorial latitudes all molecular abundances are affected by 10% or less, except for HCN (20%). This small impact is expected because the HASI profile was inferred above the Huygens landing site, which was at 10°S. In the northern latitudes, the divergence is more pronounced (as much as 20% of decrease in abundance) for some molecules (the ones with the stronger emission bands: C_2H_2 and HCN), however, even at 50°N, all the other molecular abundances vary by less than 10% whatever the initial temperature profile.

In the northern hemisphere, we find a decrease in temperature in the mesosphere (more sensitive to the seasonal insolation variations), starting from the stratopause above 0.1 mbar, where the temperature significantly decreases from the earlier to the later mission dates. The warm north polar lower mesosphere has cooled (as also suggested previously by Achterberg et al. 2011) and now we find the decrease to be about 12 K at 50°N (Figure 2(a)) and about 7 K at 30°N (Figure 2(b)) at around 250–300 km in altitude, since the beginning of the *Cassini* mission. In the mid-stratosphere below 200 km, the northern polar region initially began cooling from 2007 up to 2009, while in 2010 a slight warming is observed again at both 50°N and 30°N.

The cooling with time in the lower mesosphere (by 8 K maximum) is also witnessed at the equatorial and southern latitudes. On the contrary, in the stratosphere (lower atmospheric levels), no significant changes are found in the equatorial temperatures (Figure 2(c)) and this holds for latitudes down to

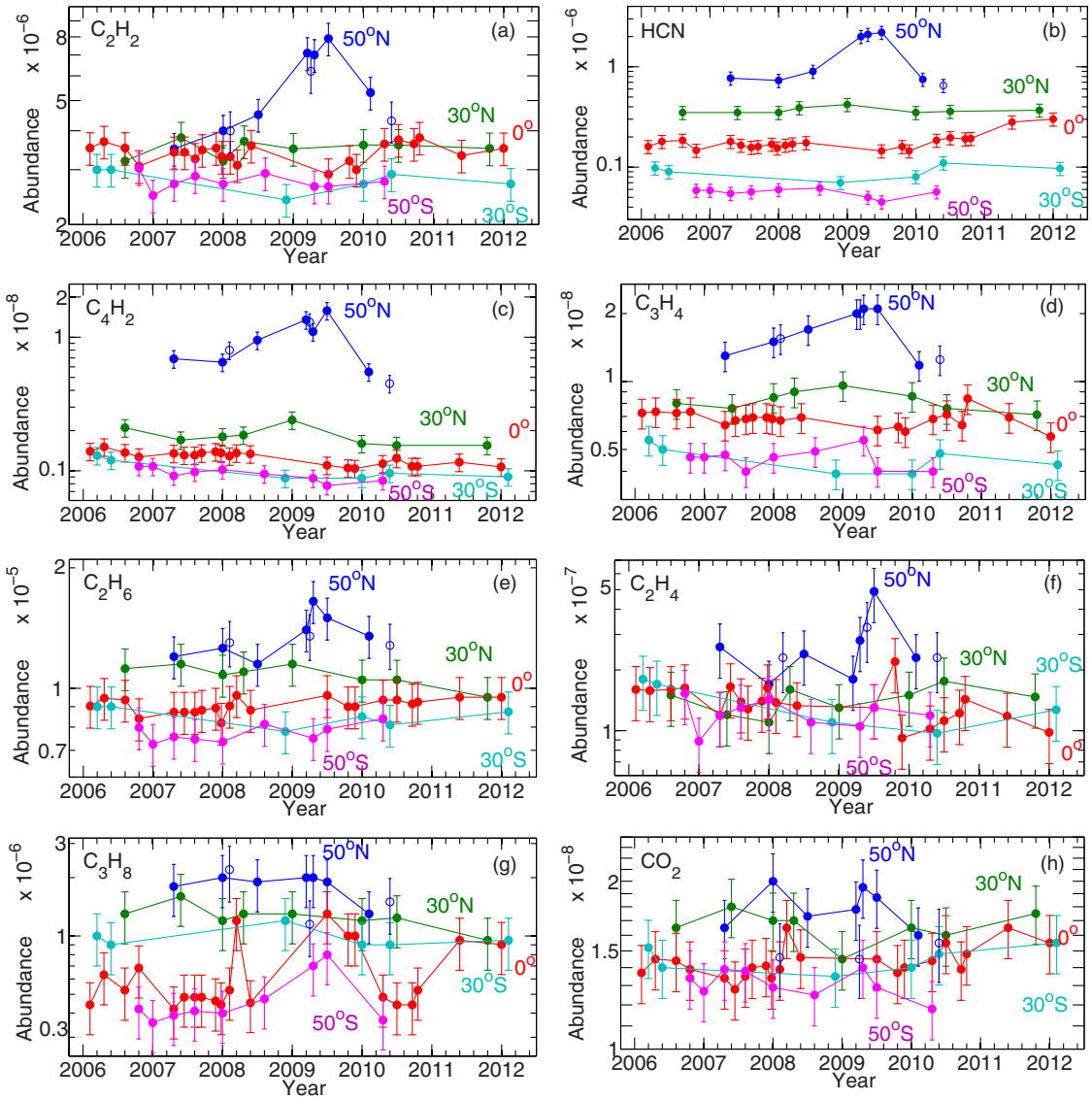

Figure 3. Time–latitude composition variations for the major trace gases of Titan's stratosphere: (a) C_2H_2, (b) HCN, (c) C_4H_2, (d) C_3H_4, (e) C_2H_6, (f) C_2H_4, (g) C_3H_8, and (h) CO_2. The latitudes investigated from 2006 to 2012 are: 50°S (violet), 30°S (light blue), equator (red), 30°N (green), and 50°N (blue). Connected filled circles are high resolution observations (0.5 cm^{-1}), while open circles are medium resolution data (2.5 cm^{-1}) for 2008, 2009, and 2010 (and sometimes coincide with the higher resolution values). The 3σ estimated error bars are indicated (see the text).

(A color version of this figure is available in the online journal.)

30°S. More to the south (50°S, Figure 2(d)), some temperature variations are observed in the stratosphere, typically 2–4 K between 1 and 10 mbar, but this is within error bars. More importantly, the general shape of the thermal structure is changing and we find the temperature gradient to be weakening, resulting in a more isothermal profile at higher latitudes with a loss of the marked stratopause present in earlier years.

These changes at northern latitudes suggest a weakening of the descending branch of the middle atmosphere meridional circulation (Achterberg et al. 2011), which implies less adiabatic heating and hence lower temperatures. Moreover, the changes in the circulation affect the distribution of aerosols (Vinatier et al. 2012a), which in turn affect the thermal structure.

4. CHEMICAL COMPOSITION CHANGES OVER THE *CASSINI* MISSION

With the thermal profiles described above injected in our radiative transfer code, we derived the abundances of the molecules from the best fits obtained of their emission bands in the Titan CIRS FP3 spectra (Figure 1(b)). We show the *Cassini*/CIRS mixing ratio inferences for Titan's gases as found above the condensation level in Figures 3(a)–(h) with the associated errors.

Since the model parameters for all these calculations are the same (in terms of calibration, methane profile, haze description model, etc.), we only consider the relative uncertainties, due to noise (rather small in our usually large averages, except for the early mission dates and sometimes in the north), the temperature profiles and any remaining uncertainties regarding some of the spectroscopic data (all within 15%). Exceptions are C_3H_8 and C_2H_4, which are affected by abundance retrieval difficulties and some insufficient laboratory spectroscopic data. In the case of C_3H_8, at 748 cm^{-1}, a major hindrance is the mixing with the C_2H_2 lines while the spectrum of C_2H_4, around 950 cm^{-1}, suffers from some electrical interference artifacts ("spikes") and also interference from C_3H_8 contribution and other emission

bands. As a consequence, these two molecules show ratios that have error bars on the order of ±30% and are not as reliable as the other inferences for the temporal or spatial variations.

At southern latitudes (50°S and 30°S, Figure 3) as well as near the equator, we find the abundances of the gaseous species to remain rather constant during the *Cassini* mission within the error bars. In general (with the exception of C_2H_4 and C_3H_8, identified as complicated molecules to process, in particular at the mid and southern latitudes), the equatorial data yield abundances higher by about 20% than the 30 or 50°S inferences (which are almost at the same level for all molecules). The mixing ratios at 30°N are in general higher than the equatorial values by 10%–20%. We found a definitive trend for increased gaseous content in the stratosphere when moving from the south to the north, and, in addition, significantly enhanced abundances during the whole mission duration at northern latitudes, observed in most cases at latitudes higher than 30°N.

At 50°N, all abundances except for CO_2 are thus enhanced with respect to 55°S and the equator, consistent with our previous work with this model (Coustenis et al. 2007, 2010) and with *Voyager 1* results (Coustenis et al. 1991; Coustenis & Bézard 1995), almost at the same season as in mid-2010 (A. Coustenis et al., in preparation). In average, and at the maximum, the 50°N values are higher than the 30°N by 20% and by 40% with respect to the equator. These enhancements appear to be greatest for the shortest-lived chemicals. This is explained by a combination of chemistry and dynamics: the vertical distributions are steepest for the shortest-lifetime species in a purely chemical model, while the presence of a circulation cell in the atmosphere, with subsidence in the polar regions (at the north pole during the period of the observations), causes the lower stratosphere to be greatly enriched in these species at the winter pole compared to the equator. The study of the temporal evolution of this enhancement in the higher northern regions within the *Cassini* mission duration, as well as changes observed with time at southern polar regions, is described by Teanby et al. (2008, 2010, 2012).

Furthermore, at 50°N, we find an indication for an increase in abundance from 2006 to mid-2009 for almost all molecules (the exceptions are propane and carbon dioxide which do not seem to vary in time at any latitude, lower double panel of Figure 3). We detect a maximum around the time of the NSE (Northern Spring Equinox, 2009 August 15) in mixing ratios with increases in abundances by about 30%–40% for C_3H_4 and C_2H_6, 50%–70% for C_2H_2 and C_4H_2, and about a factor of 2 or more for HCN and C_2H_4 (albeit with higher uncertainties for the latter) relative to the adjacent time periods in 2008 and 2010. Ethane shows variations with time only at this higher latitude. We note that C_3H_8 seems to have increased abundances around NSE, but the data analysis results for this molecule at lower latitudes are rather uncertain. The results on the increase and the reported values near April 2009 presented for C_2H_2 (7×10^{-6}) and HCN (2×10^{-6}) in these figures (just before the maximum in June 2009) are in excellent agreement with the findings of Teanby et al. (2010), as shown in their Figure 4, panels (c) and (d). Although there is a hint in their Figure 4, Teanby et al. do not yet see the increase in abundance that we report here for C_4H_2 but we are still compatible within error bars at values near 2×10^{-8} in 2009.

The observed increase in abundance for some molecules is followed by a strong decrease which reduces considerably the observed enhancement by 2010. This decrease settles in quickly, within 1–2 terrestrial years and brings the abundances back to their levels prior to the ascent. Admittedly we have so far only one high-resolution nadir selection after the NSE and one in lower resolution confirming this result, so that the finding probably requires further verification. However, both high- and low-resolution nadir data taken in the 2010–2012 period seem to support the increase and follow-up decrease.

We inferred the $^{12}C/^{13}C$ ratio in CH_4 and C_2H_2 to be 95±15 and the $^{14}N/^{15}N$ ratio in HCN to be 50±10 for the latitudes on which we investigate here as an average. The $^{12}C/^{13}C$ ratio is consistent with results reported by Vinatier et al. (2007) and Nixon et al. (2008a, 2008b) and with the terrestrial inorganic standard value (88.9; Fegley 1995). The $^{14}N/^{15}N$ ratio is also consistent with the values given by Vinatier et al. (2007) and about 4.8 times lower than the terrestrial value (272; Fegley 1995).

Since the C_2H_2 emission band at 729 cm^{-1} contains information at several altitudes through the central and wing lines, we have also tested a vertical profile predicted for Ls = 358° by the GCM models (Rannou et al. 2005), which does not match the shape of the C_2H_2 band, but is not too off with respect to the actual values.

At higher northern or southern latitudes, poleward of 70°N, the situation has dramatically changed in recent years with much stronger chemical and temperature variations (Vinatier et al. 2012b; Teanby et al. 2012) but at the latitudes considered here, we do not observe them which gives us hints as to the location and the extent of the winter polar vortex.

5. DISCUSSION OF THE RESULTS AND POSSIBLE INTERPRETATIONS

In this work, we estimate the abundances of the trace gases in Titan's stratosphere from 50°S to 50°N. We find no significant temporal variations at mid- and southern latitudes during the *Cassini* mission. We monitor and quantify the compositional enhancement at 50°N, and find indication for a maximum at the time of the Titan northern spring equinox (NSE, mid-2009), followed by a sharp decrease of the gaseous chemical content within the next Earth year or so. Our results are compatible with the findings of Teanby et al. (2010) in that we find HCN and C_2H_2 to display a rapid increase in northern latitudes up to mid-2009 while the abundances at equatorial and southern latitudes remain stable. CO_2 presents no latitudinal variations anywhere because of its long photochemical lifetime.

The peak in abundance is observed around the northern spring equinox, during which we know a rapid change in the atmosphere took place. Indeed, short-term variations observed during the *Cassini* mission can arise from changes in the circulation around the time of the equinox. The collapse of the detached aerosol layer (West et al. 2011) suggests that the dynamics during this period go through a rapid transition which should also affect the gas distribution. The rapid decrease after mid-2009, for which the most straightforward explanation is that the vortex has shrunk somewhat, would be consistent with the weakening thermal gradient we find here and that of the winds also reported by Achterberg et al. (2008, 2011) and Teanby et al. (2009b). The finding also ties into the location of the maximum temperature gradient, which appears to be moving northward over the winter/spring season (Teanby et al. 2010; Figure 3, T panel). If 50°N is emerging from the vortex core, it would cause a large reduction in the abundances, hence explaining our observations. Thus, decreasing abundances at 50°N could be

due to a weakening vortex with reduced lateral mixing across the vortex boundary (Teanby et al. 2010).

Another cause could be the spatial variations in the energy input to Titan's atmosphere (due to Titan's inclination) as a driver for changes in the advection patterns, which in turn provide a stronger variability in the latitudinal abundances of photochemical species. Changes in the solar output during the 11 year cycle can potentially affect the chemical production rates in Titan's atmosphere. On the other hand, for the time period of the *Cassini* mission, the Sun has been remarkably stable going through an extended minimum with the first weak signs of increased output observed toward the end of 2009. The chemical lifetimes in Titan's stratosphere (at 200 km) range between ∼1 year for C_2H_4 and C_3H_4 up to ∼20 years for HCN, which are longer than the timescales of some of the rapid changes observed. Thus, the temporal variability observed during the *Cassini* mission is more likely related to changes in the atmospheric circulation patterns due to progression of seasons.

We thank Nicolas Gorius, Marcia Segura, and Florence Henry for help with the data acquisition and processing during this project. We also acknowledge support from the CNES *Cassini* program.

REFERENCES

Achterberg, R. K., Conrath, B. J., Gierasch, P. J., Flasar, F. M., & Nixon, C. A. 2008, Icarus, 194, 263
Achterberg, R. K., Gierasch, P. J., Conrath, B. J., Flasar, F. M., & Nixon, C. A. 2011, Icarus, 211, 686
Coustenis, A., Achterberg, R., Conrath, B., et al. 2007, Icarus, 189, 35
Coustenis, A., & Bézard, B. 1995, Icarus, 115, 126
Coustenis, A., Bézard, B., Gautier, D., Marten, A., & Samuelson, R. 1991, Icarus, 89, 152
Coustenis, A., Jennings, D. E., Jolly, A., et al. 2008, Icarus, 197, 539
Coustenis, A., Jennings, D. E., Nixon, C. A., et al. 2010, Icarus, 207, 461
de Kok, R., Irwin, P. G. J., Teanby, N. A., et al. 2007, Icarus, 186, 354
Fegley, B. 1995, in A Handbook of Physical Constants, ed. T. Ahrens (Washington, DC: Am. Geophys. Pub.), 320
Flasar, F. M., Achterberg, R. K., Conrath, B. J., et al. 2005, Science, 308, 975
Flasar, F. M., Kunde, V. G., Abbas, M. M., et al. 2004, Space Sci. Rev., 115, 169
Flaud, J. M., Kwabia Tchana, F., Lafferty, W. J., & Nixon, C. A. 2010, Mol. Phys., 108, 699
Fulchignoni, M., Ferri, F., Angrilli, F., et al. 2005, Nature, 438, 785
Jacquinet-Husson, N., Crepeau, L., Armante, R., et al. 2011, J. Quant. Spectrosc. Radiat. Transfer, 112, 2395
Jennings, D. E., Nixon, C. A., Jolly, A., et al. 2008, Astrophys. J. Lett., 681, L109
Niemann, H. B., Atreya, S. K., Demick, J. E., et al. 2010, J. Geophys. Res., 115, E12006
Nixon, C. A., Achterberg, R. K., Vinatier, S., et al. 2008a, Icarus, 195, 778
Nixon, C. A., Jennings, D. E., Bézard, B., et al. 2008b, Astrophys. J. Lett., 681, L101
Rannou, P., Lebonnois, S., Hourdin, F., & Luz, D. 2005, Adv. Space Res., 36, 2194
Rothman, L. S., Gordon, I. E., Barbe, A., et al. 2009, JQSRT, 110, 533
Teanby, N. A., Irwin, P. G. J., de Kok, R., & Nixon, C. A. 2010, Astrophys. J. Lett., 724, L84
Teanby, N. A., Irwin, P. G. J., de Kok, R., et al. 2006, Icarus, 181, 243
Teanby, N. A., Irwin, P. G. J., de Kok, R., et al. 2007, Icarus, 186, 364
Teanby, N. A., Irwin, P. G. J., de Kok, R., et al. 2008, Icarus, 193, 595
Teanby, N. A., Irwin, P. G. J., de Kok, R., et al. 2009a, Icarus, 202, 620
Teanby, N. A., Irwin, P. G. J., de Kok, R., et al. 2009b, Phil. Trans. R. Soc. A, 367, 697
Teanby, N. A., Irwin, P. G. J., Nixon, C. A., et al. 2012, Nature, in press
Vander Auwera, J., Moazzen-Ahmadi, N., & Flaud, J.-M. 2007, Astrophys. J., 662, 750
Vinatier, S., Bézard, B., Anderson, C. M., et al. 2012b, in Titan Through Time Workshop 2012, ed. V. Cottini, C. Nicon, & R. Lorenz (NASA, FSGC), 45
Vinatier, S., Bézard, B., Fouchet, T., et al. 2007, Icarus, 188, 120
Vinatier, S., Bézard, B., Nixon, C. A., et al. 2010, Icarus, 205, 559
Vinatier, S., Rannou, P., Anderson, C. M., et al. 2012a, Icarus, 219, 5
West, R. A., Balloch, J., Dumont, P., et al. 2011, Geophys. Res. Lett., 38, L06204